Non-contact AC current measurement using vibration analysis of a MEMS piezoelectric cantilever beam

Easa AliAbbasi[1], Akbar Allahverdizadeh[1,*], Behnam Dadashzadeh[1], and Reza Jahangiri[2]

[1] *Faculty of Electrical and Computer Engineering, Department of Mechatronics Engineering, University of Tabriz, Tabriz, Iran*
[2] *Department of Mechanical Engineering, Islamic Azad University, Salmas, Iran*
[*] *Corresponding author: allahverdizadeh@tabrizu.ac.ir*

Manuscript received 14 July, 2019; revised 14 January, 2020, accepted 02 February, 2020. Paper no. JEMT-1907-1188.

This paper proposes a non-contact system to measure electrical current crossing a wire. To do so, the design and simulation of a piezoelectric cantilever beam with a tip mass are presented using mathematical modeling. The sandwich cantilever beam is composed of two piezoelectric layers and a mid-layer made up of steel. For mathematical modeling, the governing differential equation of the beam is extracted and solved by the Galerkin method. Then the output voltage is calculated for different values of external forces. The force applied to the tip mass from the magnetic field of wire is used as the external excitation force of the beam. According to the response of the output voltage, the current crossing the wire is calculated. Validation of the model is demonstrated compared to other references. In the results section, frequency response behavior and the influence of the geometric parameters on output voltage are analyzed. Appropriate values of these parameters should be used in the design process of this non-contact sensor to have an observable applied force from the current-carrying wire.

keywords: *Bimorph cantilever beam, Piezoelectric, Electrical current measurement, Forced excitation, Non-contact sensor.*

http://dx.doi.org/10.22109/jemt.2020.194283.1188

1. INTRODUCTION

Nowadays, the development of mechanical and electronic systems in very small dimensions is highly attractive for researchers and industries. Micro-electro-mechanical-systems (MEMS) technology has many applications in diverse and major industries such as automobile manufacturing, missile, chips and military. This important technology results in inefficiency increase and compactness of industrial devices. The necessity for this technology has encouraged many countries to invest in this field.

Measurement is a process that determines the amount of a physical quantity present in a context [1]. Measurement of electrical current crossing through a conductor is one of these processes. In fact, monitoring of electrical energy consumption using an effective system is highly demanded in which electrical sensor plays an important role. This sensor produces a signal from the current that can be used for control, efficiency measurement and relaying [2]. Recent studies show that users with real-time energy meters for consumption pay 3.8% less than those with standard measuring systems [3]. These sensors give the amount and also the cost of the consumed energy so that the users will dynamically monitor their consumption rate [4]. Between two main methods of electrical current measurement, direct measurement is a common and old method. High-speed measurement is essential in many cases like military sites that equipment change with missions and in cases that interrupting system may harm the sensor or the system itself. Thus, the measurement tools must be accurate and reliable and an appropriate non-contact measurement with high performance would solve the problems [3]. Scientists have proposed many non-contact procedures. Nowadays, piezoelectric sensors are being used in a wide range for measurement processes [5] and are a proper and promising choice for current measurement.

Some crystals like tourmaline, quartz, topaz and Rochelle salts produce voltage under mechanical stress. This is due to the polarization of the molecules of these materials. They are called piezoelectric materials and the effect is called the direct piezoelectric effect. The inverse effect occurs when an electric potential subject to it and the shape changes and mechanical stress appears [6, 7].

In order to use piezoelectric materials for current measurement purposes, they should be formed in cantilever beams shape. The first experiment in designing non-contact electrical current measurement sensors for household and commercial purposes was presented by Leland et al. The sensor was composed of a piezoelectric cantilever beam and a permanent magnet attached to the free end of it. The system was electrically isolated from

the current-carrying wire and the external power source was not needed [8]. Determining the exact place of permanent magnet in single and two-wire modes, which was 45 and 90 degrees, respectively, the system's results were improved [9]. Then, two different sensor configurations in four different wires were examined. The first sensor's electrodes were placed longitudinally all over the conductor, but the second ones' were placed in half of the length of it. The resonant frequency was 1.23 kHz and 960 Hz, respectively. The variety in micro-magnets construction helped to manufacture bigger and heavier magnet in second sensor so that the frequency response was reduced [10]. Another MEMS DC electric current sensor with the same concept was designed and proposed by Isagawa et al. Being non-drive, non-contact and measuring currents from 0.04 A to 10 A was the characteristics of it [11]. This piezoelectric cantilever based current sensor could be improved by attaching permanent magnet in the top and bottom of the cantilever beam head. An electrical current control system with this property was presented by Qiliang et al. It could be enabled wirelessly and also could be retrofitted to sub-meter existing buildings in order to have individual cost monitoring [12]. A new method based on piezoelectric and magnetostrictive materials was established by He et al. [13]. The magnetostrictive FCEA layer was used as a shim and the PZT layer was placed on it. Also, a tunable mass was fixed at the end of the cantilever beam, so as to let the beam vibrate in the frequency of crossing current. The magnetization of the magnetostrictive layer in the longitudinal direction in the presence of a magnetic field of a conductor caused the piezoelectric layer to polarize in a thickness direction. The sensor's functional range was from 1 A_{rms} to 10 A_{rms} and in 50 Hz resonant frequency.

In this paper, a bimorph piezoelectric cantilever beam is designed for non-contact electrical current measurements. It is obvious that every electrical current-carrying conductor has a magnetic field around itself and produces a magnetic force in which by measuring this force and using electromagnetic equations, the crossing current could be calculated. According to this, a mathematical model for a piezoelectric cantilever beam with a permanent magnet attached to its free end is presented. Coupling of the magnetic field of the wire with the magnet's magnetic field will generate a relationship between the conductor and the cantilever beam, which can vibrate the beam and accordingly polarize the piezoelectric layers. Though, based on the direct piezoelectric effect, the output voltage will be generated in the fixed end of the beam. Unlike previous studies in using piezoelectric cantilever beams for magnetic field sensing approaches, distributed-parameter predictions is used in this paper instead of lumped-parameter predictions. This is due to the fact that the error of the lumped-parameter model in predicting the relative motion of the beam is 35% greater than the distributed-parameter model [14].

2. MAGNETIC FIELD OF A CURRENT-CARRYING WIRE

As shown in Fig. 1, a magnetic field is generated when electric current flows through a conductor, as introduced by Oersted [15]. The contour of the magnetic field will vary depending on the shape of the conductor. Obviously, the magnetic field takes the form of concentric circles if the conductor is a wire. It is stronger in the area closer to the wire and its direction depends on the direction of the current that produces the field. The Lorentz Force is applied to a current in a magnetic field since an electrical current in a wire consists of moving electrons. Thus, the force exerted by the current crossing the wire on the

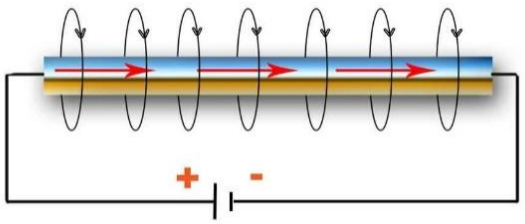

Fig. 1. Illustration of the magnetic field around a current carrying wire.

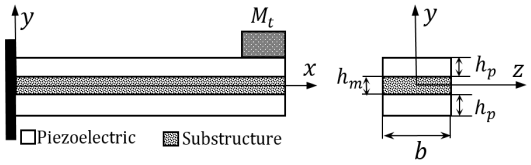

Fig. 2. Bimorph piezoelectric cantilever beam presentation.

permanent magnet, which is attached to the free end of the piezoelectric cantilever beam, is [16]:

$$\vec{F} = \vec{i} L \times \vec{B} \tag{1}$$

where, F is the force in Newton, B is the strength of the magnetic field in Tesla, i is the electrical current in Ampere, and L is the length of the wire through the magnetic field in meters. It is worth noting that, magnetic field decreases with inverse-square of distance. According to Ampere's Law, the magnetic field is calculated using (2) in which r represents wire's radius and the permeability coefficient is $\mu_0 = 4\pi \times 10^{-7} T.m/A$.

$$B = \frac{\mu_0 I}{2\pi r} \tag{2}$$

3. ANALYTICAL MODELING OF THE BIMORPH PIEZOELECTRIC CANTILEVER BEAM

The procedure of calculating the magnetic force applied from the magnetic field of current-carrying wire is presented in this section. To obtain the equation of the produced output voltage of the piezoelectric cantilever beam as a result of the applied forces, a bimorph cantilever beam is supposed, as shown in Fig. 2. In bimorph piezoelectric cantilever beams, the layers could be connected in series or parallel. A parallel connection is considered in our model.

A. Governing equation of motion of the beam

For an undamped cantilever beam, the following equation can be written [17]:

$$YI \frac{\partial^4 w(x,t)}{\partial x^4} + m \frac{\partial^2 w(x,t)}{\partial t^2} = 0 \tag{3}$$

in which, YI, m, and w represent bending stiffness, mass per unit length and transverse displacement at the free end of the beam, respectively. Introducing mechanical damping to (3) that is composed of viscous air damping coefficient, c_s and strain rate

damping coefficient, c_a, one can derive the equation of motion in the presence of damping effects as [14]:

$$YI\frac{\partial^4 w(x,t)}{\partial x^4}+c_sI\frac{\partial^5 w(x,t)}{\partial x^4\partial t}+c_a\frac{\partial w(x,t)}{\partial t}+m\frac{\partial^2 w(x,t)}{\partial t^2}=0 \quad (4)$$

where, I is the equivalent moment of inertia. To measure electrical current, the magnetic field of the wire should be in interaction with a beam on which a permanent magnet is attached to the free end as proof mass. By adding this proof mass to the free end of the beam, a magnetic force would affect the beam and the equation of motion would be changed as (5).

$$-\frac{\partial^2 M(x,t)}{\partial x^2}+c_sI\frac{\partial^5 w(x,t)}{\partial x^4\partial t}+c_a\frac{\partial w(x,t)}{\partial t}+m\frac{\partial^2 w(x,t)}{\partial t^2}=f(t) \quad (5)$$

In the above equation, M is the bending moment which could be calculated as below:

$$M(x,t)=b\left(\int_{-h_p-h_m/2}^{-h_m/2}T_pzdz+\int_{-h_m/2}^{h_m/2}T_mzdz+\int_{h_m/2}^{h_p+h_m/2}T_pzdz\right) \quad (6)$$

where b, h, and T represent beam width, beam thickness and stress component in x-direction, respectively and p and m indicate piezoelectric layer and non-piezoelectric layer. So, (7) and (8) could be written for axial stresses as:

$$T_m=Y_mS_m \quad (7)$$

$$T_p=C_{11}^ES_p-e_{31}E_3 \quad (8)$$

In these equations, Y and c_E show elastic modulus of piezoelectric and mid-layer and S, e, and E represent axial strain components in each layer, piezoelectric stress constant and electric field, respectively. Equation (9) is found suitable for axial strain.

$$S(x,z,t)=-z\frac{\partial^2 w(x,t)}{\partial x^2} \quad (9)$$

Substituting (7) and (8) into (6) and integrating it results in (10), which presents the relation between bending moment and backward coupling coefficient.

$$M(x,t)=-YI\frac{\partial^2 w(x,t)}{\partial x^2}+\vartheta v(t)\left[H(x)-H(x-L)\right] \quad (10)$$

In this equation, H is Heaviside function, $v(t)$ is voltage, L is the length of the beam and the bending stiffness YI, backward coupling coefficient ϑ, and mass of the beam are obtained as:

$$YI=\frac{2b}{3}\left\{Y_m\frac{h_m^3}{8}+c_{11}^E\left[\left(h_p+\frac{h_m}{2}\right)^3-\frac{h_m^3}{8}\right]\right\} \quad (11)$$

$$\vartheta=\frac{e_{31}b}{h_p}\left[\left(h_p+\frac{h_m}{2}\right)^2-\frac{h_m^2}{4}\right] \quad (12)$$

$$m=b\left(2\rho_ph_p+\rho_mh_m\right) \quad (13)$$

Substituting (10) in (5) would present the final governing equation of motion of the beam.

$$YI\frac{\partial^4 w(x,t)}{\partial x^4}+c_sI\frac{\partial^5 w(x,t)}{\partial x^4\partial t}+c_a\frac{\partial w(x,t)}{\partial t}+m\frac{\partial^2 w(x,t)}{\partial t^2}-\vartheta v(t)\left[\frac{d\delta(x)}{dx}-\frac{d\delta(x-L)}{dx}\right]=f(t) \quad (14)$$

B. Solving the equation of motion

In order to solve equation (14), Galerkin method is utilized. It represents the amount of transverse deflection in time t and longitudinal position x. It is presented as (15) and $\Phi_i(x)$ and $\eta_i(t)$ show mass-normalized eigenfunction of the ith vibration mode and modal mechanical coordinate expression, respectively.

$$w(x,t)=\sum_{i=1}^{\infty}\Phi_i(x)\eta_i(t) \quad (15)$$

In calculating the mass-normalized eigenfunction, one should consider the proof mass M_t, because it would affect the whole response [14].

$$\Phi_i(x)=A_i\left[\cos\frac{\lambda_i}{L}x-\cosh\frac{\lambda_i}{L}x+\varsigma_i\left(\sin\frac{\lambda_i}{L}x-\sinh\frac{\lambda_i}{L}x\right)\right] \quad (16)$$

where,

$$\varsigma_i=\frac{\sin\lambda_i-\sinh\lambda_i+\lambda_i\frac{M_t}{mL}\left(\cos\lambda_i-\cosh\lambda_i\right)}{\cos\lambda_i-\cosh\lambda_i+\lambda_i\frac{M_t}{mL}\left(\sin\lambda_i-\sinh\lambda_i\right)} \quad (17)$$

A_i is modal amplitude constant in (16), which is evaluated by normalizing (18) and (19). In these equations, I_t and δ_{is} are the proof mass moment of inertia in $x=L$ and Kronecker delta, respectively.

$$\int_0^L\Phi_s(x)m\Phi_i(x)dx+\Phi_s(L)M_t\Phi_i(L)+\left[\frac{d\Phi_s(x)}{dx}I_t\frac{d\Phi_i(x)}{dx}\right]_{x=L}=\delta_{is} \quad (18)$$

$$\int_0^L\Phi_s(x)YI\frac{d^4\Phi_i(x)}{dx^4}dx-\left[\Phi_s(x)YI\frac{d^3\Phi_i(x)}{dx^3}\right]_{x=L}+\left[\frac{d\Phi_s(x)}{dx}YI\frac{d^2\Phi_i(x)}{dx^2}\right]_{x=L}=\omega_i^2\delta_{is} \quad (19)$$

Also, ω_i is the undamped natural frequency of the ith vibration mode which could be written as:

$$\omega_i=\lambda_i^2\sqrt{\frac{YI}{mL^4}} \quad (20)$$

The eigenvalue λ_i is calculated as:

$$1+\cos\lambda\cosh\lambda+\lambda\frac{M_t}{mL}\left(\cos\lambda\sinh\lambda-\sin\lambda\cosh\lambda\right)-\frac{\lambda^3I_t}{mL^3}\left(\cos\lambda\sinh\lambda+\sin\lambda\cosh\lambda\right)+\frac{\lambda^4M_tI_t}{m^2L^4}\left(1-\cos\lambda\cosh\lambda\right)=0 \quad (21)$$

B.1. Analysis of electric circuit for a piezoceramic cantilever beam under mechanical deflection

At first, the electrostatic behavior of a thin layer will be discussed, which would lead to the derivation of the piezoelectric governing equation. Only axial strain is considered and because of that, electric displacement is written as follows:

$$D_3=e_{31}S_p+\varepsilon_{33}^sE_3 \quad (22)$$

where, ε_{33} is the permittivity component in constant strain. Gauss's law is written as (23) in which n and R_L represent the unit outward normal and output resistance, respectively. Also, the integration is done over the electrode area A and D shows the vector of electric displacement components.

$$\frac{d}{dt}\left(\int_A D.ndA\right)=\frac{v(t)}{R_L} \quad (23)$$

The relation between the electrical field and electrical voltage is $E_3 = -v(t)/h_p$ in parallel mode. Considering (9) and substituting (22) in (23), the governing equation of the output voltage of the thin piezoelectric layer would be as:

$$\frac{\varepsilon_{33}^{s} bL}{h_p}\frac{dv(t)}{dt} + \frac{v(t)}{R_L} + e_{31}h_{pc}b\int_0^L \frac{\partial^3 w(x,t)}{\partial x^2 \partial t}dx = 0 \quad (24)$$

where, h_{pc} shows the distance between the neutral axis and the center of each piezoelectric layer. It is calculated as:

$$h_{pc} = (h_p + h_m)/2 \quad (25)$$

The output voltage could be presented by substituting (15) in (24).

$$\frac{\varepsilon_{33}^{s} bL}{h_p}\frac{dv(t)}{dt} + \frac{v(t)}{R_L} + \sum_{i=1}^{\infty}\kappa_i \frac{d\eta_i(t)}{dt} = 0 \quad (26)$$

k_i is modal coupling term in the electrical circuit and could be calculated as follows:

$$\kappa_i = -e_{31}h_{pc}b\int_0^L \frac{d^2\Phi_i(x)}{dx^2}dx = -e_{31}h_{pc}b\left.\frac{d\Phi_i(x)}{dx}\right|_{x=L} \quad (27)$$

Fig. 3A shows the schematic view of the equivalent electrical circuit of the piezoelectric cantilever beam. According to Kirchhoff's current law, (28) could be derived and equating it with (26) brings out the terms of internal capacitance and dependent current source, which are presented in (29) and (30), respectively.

$$C_p\frac{dv(t)}{dt} + \frac{v(t)}{R_L} - i_p(t) = 0 \quad (28)$$

$$C_p = \varepsilon_{33}^{s} bL/h_p \quad (29)$$

$$i_p(t) = -\sum_{i=1}^{\infty}\kappa_i\frac{d\eta_i(t)}{dt} \quad (30)$$

The mechanical equation of motion in modal coordinates is derived by substituting (15) into (14) as following:

$$\frac{d^2\eta_i(t)}{dt^2} + 2\zeta_i\omega_i\frac{d\eta_i(t)}{dt} + \omega_i^2\eta_i(t) - \chi_i v(t) = f_i(t) \quad (31)$$

where, the electromechanical coupling term, χ_i is as:

$$\chi_i = \vartheta\left.\frac{d\Phi_i(x)}{dx}\right|_{x=L} \quad (32)$$

As the excitation force from the magnetic field of current-carrying wire is time-variant, the modal mechanical force term should be written as (33). F_i is the amplitude of the force.

$$f_i(t) = F_i e^{j\omega t} \quad (33)$$

Using Kirchhoff's law and the schematic of the equivalent circuit of a cantilever beam in the parallel mode shown in Fig. 3B, one can write the governing equation of dynamical output voltage as follows:

$$C_p\frac{dv(t)}{dt} + \frac{v(t)}{2R_L} - i_p(t) = 0 \quad (34)$$

Placing the harmonic solutions for $\eta_i(t)$ and $v(t)$ and also by solving the equation governing cross-sectional movements of the beam, the steady-state voltage response is:

$$v(t) = \frac{\sum_{i=1}^{\infty}\frac{-j\omega\kappa_i F_i}{\omega_i^2 - \omega^2 + j2\zeta_i\omega_i\omega}}{\frac{1}{2R_L} + j\omega C_p + \sum_{i=1}^{\infty}\frac{-j\omega\kappa_i\chi_i}{\omega_i^2 - \omega^2 + j2\zeta_i\omega_i\omega}}e^{j\omega t} \quad (35)$$

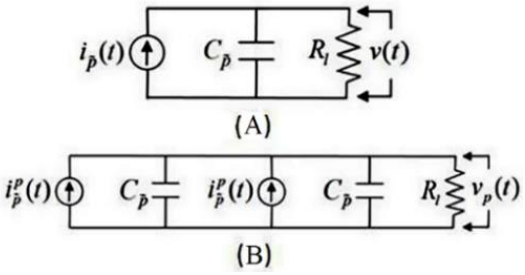

Fig. 3. Schematic of an equivalent circuit for bimorph cantilever beam (A) by considering one dependent current source and (B) by considering two dependent current sources.

The above equation is valid for all frequencies. Simplifying this equation, output voltage could be reduced to (36) by using the effect of the first vibrational mode shape of the beam.

$$v(t) = \frac{j2\omega R_L\kappa_i F_i}{(1 + j2\omega R_L C_p)\left(\omega_i^2 - \omega^2 + j2\zeta_i\omega_i\omega\right) + j2\omega R_L\kappa_i\chi_i}e^{j\omega t} \quad (36)$$

4. FREQUENCY ANALYSIS OF THE BEAM RESONANCE

Resonant or natural frequency of a system is a frequency at which it vibrates freely. Although it is possible to set up vibrations at other frequencies, they require much more energy and constant input to maintain compared to the resonant frequency. In addition, in this frequency, maximum output power density is obtained. After selecting materials, the resonant frequency depends on dimensions and the proof mass. Equation (37) is the frequency formula used for cantilever beams in order to estimate the amount of proof mass [16, 18, 19].

$$f_i = \frac{v_i^2}{2\pi}\sqrt{\frac{0.236D_p b}{\left(L - \frac{l_m}{2}\right)^3[m_e + M_t]}} \quad (37)$$

In above equation, f_i is the ith mode resonant frequency, l_m is the length of the proof mass, v_i is the ith mode eigenvalue that in first mode is 1.875 volts, D_p is the curvature modulus and m_e is the effective mass of the cantilever beam at the middle of the proof mass and is as follows:

$$m_e = 0.236mb\left(L - \frac{l_m}{2}\right) + mb\frac{l_m}{2} \quad (38)$$

For a bimorph cantilever beam, curvature modulus is as:

$$D_p = \frac{2Y_m c_{11}^E h_p^3}{3} + c_{11}^E h_m h_p^2 + \frac{c_{11}^E h_m^2 h_p}{2} + \frac{h_m^3 Y_m}{12} \quad (39)$$

5. MATHEMATICAL MODEL VALIDATION

In order to validate the mathematical model, it is compared with research which is established in 2009 [20]. The paper presented the analysis of a bimorph piezoelectric cantilever beam for energy harvesting. Results with the same input are compared, as shown in Fig. 4. It is obvious that they have a good coincidence.

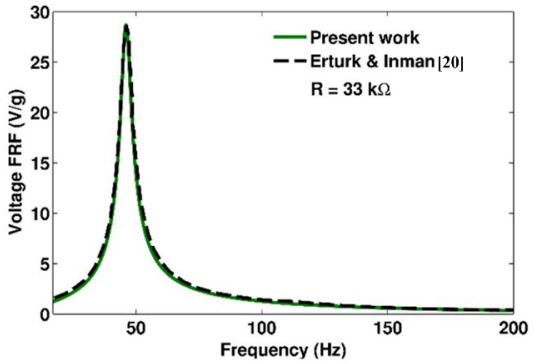

Fig. 4. Validation of results with reference [20].

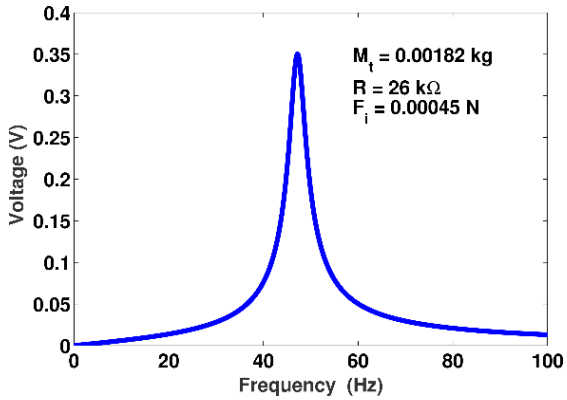

Fig. 5. Frequency response of the beam.

Table 1. Geometrical and material parameters

Parameter	PIEZOELECTRIC	Steel
Layer's length (mm)	20	20
Layer's width (mm)	14	14
Layer's height (mm)	0.06	0.04
Mass of permanent magnet (g)	1.82	
Density ($kg.m^{-3}$)	7750	7850
Elastic modulus (GPA)	62	200
Dielectric constant ($pm.V^{-1}$)	-171	-

6. RESULTS

In this analysis, the piezoelectric material is PZT-5A and the mid-layer is steel. There were two considerations in selecting proper piezoelectric material. PZT composites present piezoelectric properties very well [21]. As well, these composites have a great operation in low noise [22]. In addition, PZT-A type composites have enhanced output voltage compared to PZT-H types [23].

The length, the width and the thickness of the beam are 20 *mm*, 14 *mm*, and 0.016 *mm*, respectively. These dimensions are selected because A) the magnetic field around a current-carrying wire is very weak and to sense this field, the dimensions must be in a very low range and B) the dimensions should be in relation to fix frequency response of the beam on the desired value. The parameters shown in Table 1 are used in simulations.

Using the equations of Section 2, the force applied from the magnetic field of the wire can be calculated. For an AC current with 15 *A*, the amplitude of the applied force would be 0.00045 *N*. Fig. 5 shows the frequency response of the beam by considering the output resistance as 26 $k\Omega$. It is obvious that in 47 *kHz*, the maximum output voltage is generated. In the current measurement process with a piezoelectric cantilever beam, the output voltage of the beam must be declared exactly. Applying a force equivalent to 15 *A* current, output voltage in time range is presented in Fig. 6. Also, the output voltage is plotted in two frequencies. Fig. 6A shows the output voltage in the resonance frequency that is obtained from Fig. 5 as 47.04 *Hz* and Fig. 6B shows the voltage in 50 *Hz*. It is obvious from Fig. 6A that after 0.38 *s*, the amplitude of the output voltage reaches its maximum value and remains constant at 0.35 *V*. As illustrated in Fig. 6B, by changing the vibration frequency of the beam, the output voltage reaches its steady response after 0.30 *s*, but the voltage amplitudes are lower than the value obtained in resonance frequency.

In response analyses of the beam, the designer should consider many aspects because the change of some parameters of the beam may affect both frequency response and output voltage significantly. One important parameter is the length of the beam. In Fig. 7A, the changes in natural frequency with respect to different values of length is observed. It is obvious that increasing the length lowers the frequency. In addition, output voltage changes by length. Frequency response of the beam is plotted for 5 different values of length in Fig. 7B. It shows that by increasing the length, resonant frequency decreases and the amplitude of output voltage increases.

Also, the width of the beam has large effects on the beam responses. Keeping other parameters constant, variations of the natural frequency with respect to the beam width is illustrated in Fig. 8A. It is shown that by increasing the value of the width, natural frequency increases, too. This concept is valid in output voltage analysis. In addition, width variation affects the output voltage amplitude directly that is plotted in Fig. 8B.

In designing piezoelectric cantilever beams, it is very important to select some of the beam parameters proportional to each other. Both the piezoelectric layer and non-piezoelectric layer ratio and the ratio of proof mass to beam mass are very important. As presented in Fig. 9A, the ratio of layers height has a prominent impact in natural frequency. It can be seen that the natural frequency increases by increasing this ratio. This impact is clearly presented in Fig. 9B in which by increasing the ratio of proof mass to beam mass, the natural frequency of the beam decreases.

Frequency response with respect to output resistance and the amplitude of applied force are illustrated in Fig. 10A and Fig. 10B. These two parameters have no effect on beam resonant frequency, but they only can change output voltage amplitude. Based on Ohm's law, resistance has a direct relation with voltage, which is shown in Fig. 10A. As well, based on (36), the output voltage varies with applied force changes directly and increasing the force causes an increase in voltage that is shown in Fig. 10B.

The ratio of the mass of permanent magnet to beam mass should be evaluated that Fig. 11 shows this fact clearly. This ratio could change both resonant frequency and output voltage simultaneously. It would be observed that by increasing this ratio, the resonant frequency decreases, but output voltage increases.

The last point to be considered is the impact of the damping

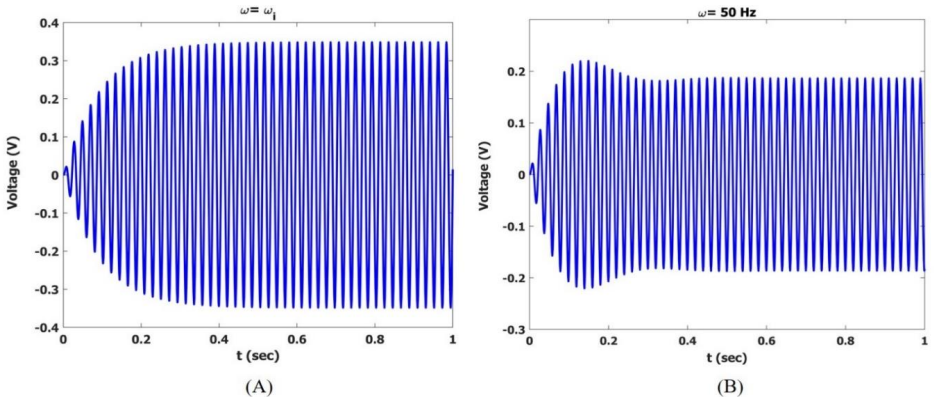

Fig. 6. Output voltage of the beam in (A) Resonance frequency (B) 50 Hz.

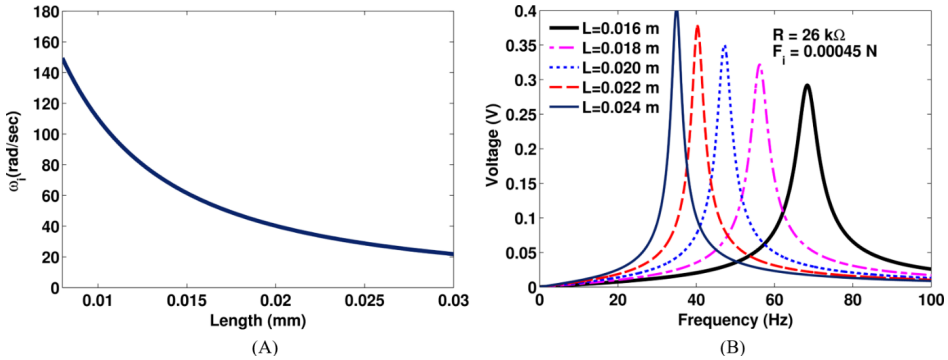

Fig. 7. A) Natural frequency vs. different values of beam's length (B) Beam's frequency response with respect to different values of length.

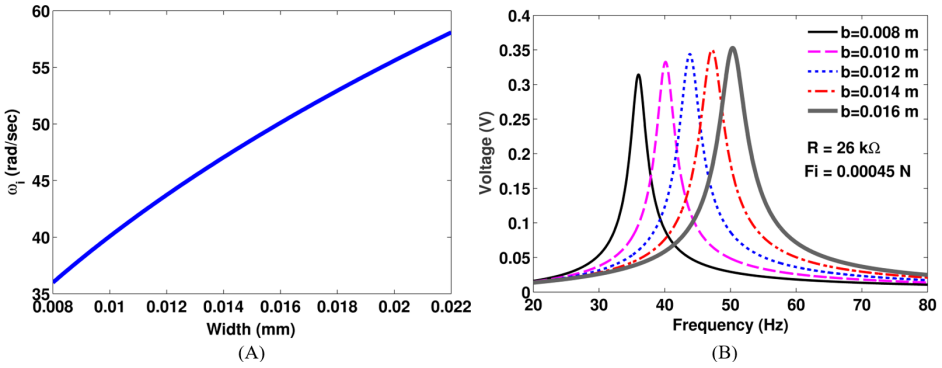

Fig. 8. (A) Natural frequency changes vs. width (B) Beam frequency response with respect to different values of width.

ratio on the output voltage. Assuming the forced excitation and output resistance, as illustrated in previous calculations, increasing the damping ratio would decrease the output voltage. This is presented in Fig. 12.

7. CONCLUSION

A mathematical model for a bimorph cantilever beam, in order to measure the current of a wire with a non-contact method, is presented in this paper. Using the numerical results, the changes of different geometrical parameters of the sensor and their effects on frequency response and output voltage were studied. Furthermore, the effect of changing proof mass on output voltage for different excitation frequencies was illustrated. As the main contribution, the applicability of the piezoelectric cantilever beam in the non-contact electrical current measurement system was shown. Due to the weak magnetic field of the wire, the beam parameters should be selected accurately.

According to the results, the resonance frequency of the beam is 47.04 *Hz* and increasing both the length and the width of the beam would result in an increase of the output voltage. However, an increase in length and width will decrease and increase the resonance frequency, respectively. In addition, the resistor value is 26 $k\Omega$ that increasing it would increase the output voltage. According to numerical results, 15 A current

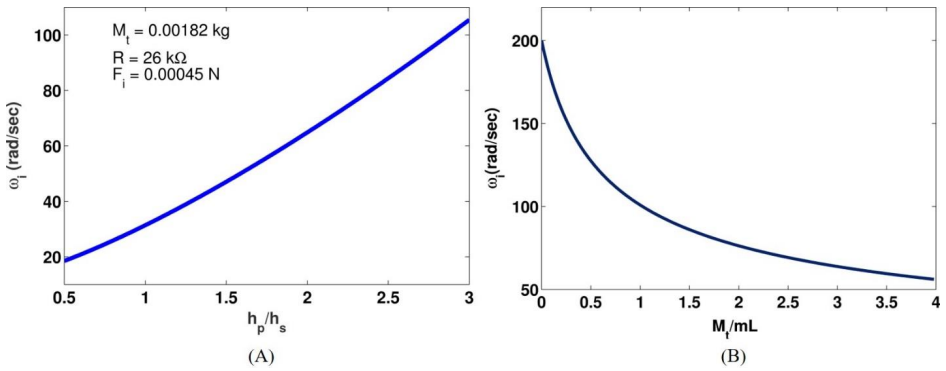

Fig. 9. Natural frequency changes for (A) different thickness ratios (B) different ratios of proof mass to beam mass.

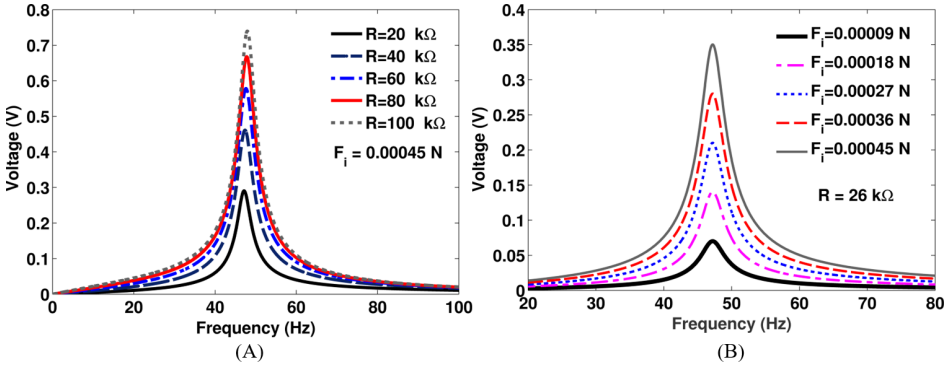

Fig. 10. Frequency response (A) for different resistances and (B) for different force amplitude.

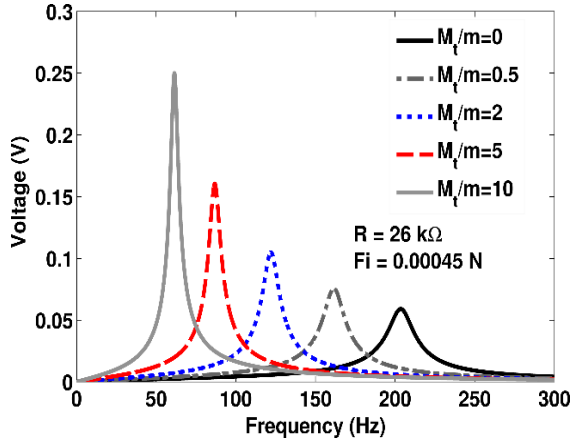

Fig. 11. Frequency response for different mass ratios.

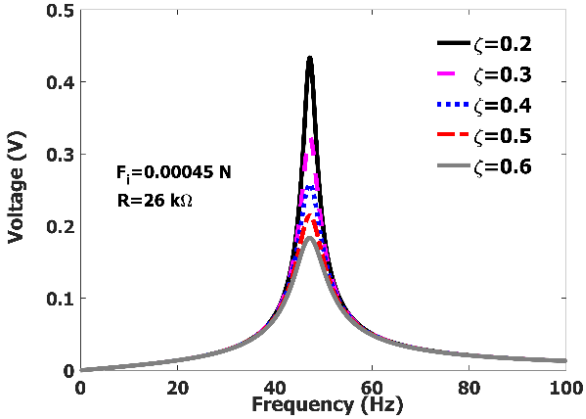

Fig. 12. Frequency response for different damping ratios.

crossing the wire generates 0.00045 N force and also 0.35 V output voltage. Therefore, the designed sensor has an acceptable sensitivity.

REFERENCES

1. F. S. Roberts, Measurement Theory: Cambridge University Press, 1985.
2. A. S. Katkar, E. T. Toppo, and M. Satarkar, "Novel approach for measurement of high current by piezoelectric technology," in 5th International Conference on Power Electronics (IICPE), India, pp. 1-6, 2012.
3. J. S. Donnal and S. B. Leeb, "Noncontact Power Meter," Sensors Journal, IEEE, vol. 15, pp. 1161-1169, 2015.
4. E. J. Moniz, "Engaging Electricity Demand," presented at the MIT Study on the Future of the Electric Grid, Cambridge, MA, USA, 2011.
5. S. S. Rao and M. Sunar, "Piezoelectricity and its use in disturbance sensing and control of flexible structures: a survey," Applied mechanics reviews, vol. 47, pp. 113-123, 1994.
6. J. Yang, An introduction to the theory of piezoelectricity vol. 9: Springer Science & Business Media, 2004.
7. A. Carazo and R. i. T. Bosch, "Novel piezoelectric transducers for high voltage measurements," Doctoral, d'Enginyeria Elèctrica, Universitat Politècnica de Catalunya, Barcelona, 2000.

8. E. Leland, P. Wright, and R. White, "Design of a MEMS passive, proximity-based AC electric current sensor for residential and commercial loads," in Procedings of PowerMEMS, Freiburg Germany, pp. 77-80, 2007.
9. E. S. Leland, P. Wright, and R. M. White, "A MEMS AC current sensor for residential and commercial electricity end-use monitoring," Journal of Micromechanics and Microengineering, vol. 19, p. 94018, 2009.
10. E. S. Leland, C. T. Sherman, P. Minor, R. M. White, and P. K. Wright, "A new MEMS sensor for AC electric current," in Sensors, Kona, HI, pp. 1177-1182, 2010.
11. K. Isagawa, D. F. Wang, T. Kobayashi, T. Itoh, and R. Maeda, "Development of a MEMS DC electric current sensor applicable to two-wire electrical appliance cord," in International Conference on Nano/Micro Engineered and Molecular Systems (NEMS), pp. 932-935, 2011.
12. Q. Xu, M. Seidel, I. Paprotny, R. M. White, and P. K. Wright, "Integrated centralized electric current monitoring system using wirelessly enabled non-intrusive ac current sensors," in IEEE Sensors, Limerick, Ireland, pp. 1998-2001, 2011.
13. W. He, P. Li, Y. Wen, and C. Lu, "A self-powered high sensitive sensor for AC electric current," in Sensors, pp. 1863-1865, 2011.
14. A. Erturk and D. J. Inman, Piezoelectric energy harvesting: John Wiley & Sons, 2011.
15. S. Kim, "Low power energy harvesting with piezoelectric generator," University of Pittsburgh, 2002.
16. D. Shen, J.-H. Park, J. H. Noh, S.-Y. Choe, S.-H. Kim, H. C. Wikle, et al., "Micromachined PZT cantilever based on SOI structure for low frequency vibration energy harvesting," Sensors and actuators A: physical, vol. 154, pp. 103-108, 2009.
17. S. S. Rao, Vibration of continuous systems: John Wiley & Sons, 2007.
18. J. W. Yi, W. Y. Shih, and W.-H. Shih, "Effect of length, width, and mode on the mass detection sensitivity of piezoelectric unimorph cantilevers," Journal of applied physics, vol. 91, pp. 1680-1686, 2002.
19. X. Li, W. Y. Shih, I. A. Aksay, and W. H. Shih, "Electromechanical Behavior of PZTBrass Unimorphs," Journal of the American Ceramic Society, vol. 82, pp. 1733-1740, 1999.
20. A. Erturk and D. J. Inman, "An experimentally validated bimorph cantilever model for piezoelectric energy harvesting from base excitations," Smart materials and structures, vol. 18, p. 025009, 2009.
21. Z. De-Qing, W. Da-Wei, Y. Jie, Z. Quan-Liang, W. Zhi-Ying, and C. Mao-Sheng, "Structural and electrical properties of PZT/PVDF piezoelectric nanocomposites prepared by cold-press and hot-press routes," Chinese Physics Letters, vol. 25, p. 4410, 2008.
22. L. Capineri, L. Masotti, V. Ferrari, D. Marioli, A. Taroni, and M. Mazzoni, "Comparisons between PZT and PVDF thick films technologies in the design of low-cost pyroelectric sensors," Review of Scientific Instruments, vol. 75, pp. 4906-4910, 2004.
23. M. J. Ramsay and W. W. Clark, "Piezoelectric energy harvesting for bio-MEMS applications," in SPIE's 8th Annual International Symposium on Smart Structures and Materials, pp. 429-438, 2001.